

Article

An Unbiased Screen Identifies DEP-1 Tumor Suppressor as a Phosphatase Controlling EGFR Endocytosis

Gabi Tarcic,^{1,6} Shlomit K. Boguslavsky,^{1,6,7} Jean Wakim,¹ Tai Kiuchi,^{2,3} Angela Liu,⁴ Felicia Reinitz,⁴ David Nathanson,⁴ Takamune Takahashi,⁵ Paul S. Mischel,⁴ Tony Ng,² and Yosef Yarden^{1,*}

¹Department of Biological Regulation, The Weizmann Institute of Science, Rehovot 76100, Israel

²Richard Dimbleby Department of Cancer Research, Randall Division of Cell and Molecular Biophysics, and Division of Cancer Studies, King's College, London WC2R 2LS, UK

³Guy's School of Medicine, Breakthrough Breast Cancer Research Unit, Guy's Hospital, King's Health Partners Academic Health Sciences Centre (AHSC), London SE1 9RT, UK

⁴Department of Pathology and Laboratory Medicine, David Geffen School of Medicine, University of California, Los Angeles, Los Angeles, CA 90095, USA

⁵Vanderbilt University Medical Center, Nashville, TN 37232, USA

Summary

Background: The epidermal growth factor (EGF) stimulates rapid tyrosine phosphorylation of the EGF receptor (EGFR). This event precedes signaling from both the plasma membrane and from endosomes, and it is essential for recruitment of a ubiquitin ligase, CBL, that sorts activated receptors to endosomes and degradation. Because hyperphosphorylation of EGFR is involved in oncogenic pathways, we performed an unbiased screen of small interfering RNA (siRNA) oligonucleotides targeting all human tyrosine phosphatases.

Results: We report the identification of PTPRK and PTPRJ (density-enhanced phosphatase-1 [DEP-1]) as EGFR-targeting phosphatases. DEP-1 is a tumor suppressor that dephosphorylates and thereby stabilizes EGFR by hampering its ability to associate with the CBL-GRB2 ubiquitin ligase complex. DEP-1 silencing enhanced tyrosine phosphorylation of endosomal EGFRs and, accordingly, increased cell proliferation. In line with functional interactions, EGFR and DEP-1 form physical associations, and EGFR phosphorylates a substrate-trapping mutant of DEP-1. Interestingly, the interactions of DEP-1 and EGFR are followed by physical segregation: whereas EGFR undergoes endocytosis, DEP-1 remains confined to the cell surface.

Conclusions: EGFR and DEP-1 physically interact at the cell surface and maintain bidirectional enzyme-substrate interactions, which are relevant to their respective oncogenic and tumor-suppressive functions. These observations highlight the emerging roles of vesicular trafficking in malignant processes.

Introduction

The balanced action of protein tyrosine kinases (PTKs) and protein tyrosine phosphatases (PTPs) is considered a major

switch of many signal transduction pathways [1]. Interestingly, both families include transmembrane receptor-like enzymes, namely receptor tyrosine kinases (RTKs) and the less understood receptor-like PTPs (RPTPs). This divergence is exemplified by the epidermal growth factor receptor (EGFR) [2]. Upon EGF binding and subsequent structural alterations, receptor dimers are stabilized, thereby allowing activation of the intrinsic kinase domain and self-phosphorylation. Concomitant with transfer of active receptors from the plasma membranes to endosomes, phosphorylated tyrosine residues of EGFR act as docking sites for adaptors and enzymes that activate either stimulatory pathways, such as the mitogen-activated protein kinase (MAPK), or inhibitory cascades, like the CBL ubiquitin ligase. By ubiquitylating EGFR, CBL instigates a process mediated by four endosomal sorting complexes (ESCRTs), culminating in lysosomal degradation of EGFR [3].

Several PTPs have been identified as candidate regulators of EGFR. For instance, EGFR phosphorylation was reduced upon inducible expression of RPTP-sigma [4]. Other examples include PTPN1/PTP1B [5, 6] and PTPN2/TCPTP [7]. Notably, PTP1B-mediated dephosphorylation of EGFR requires receptor endocytosis [8]. On the other hand, TCPTP is activated at the plasma membrane by a collagen-binding integrin to negatively regulate EGFR [9]. Finally, forced coexpression of EGFR and various RPTPs enabled identification of RPTP-kappa as an enzyme capable of reducing EGFR phosphorylation [10].

The present study employed a small interfering RNA (siRNA) library representing all human PTPs to identify PTPs able to catalytically interact with EGFR. The screen identified a candidate EGFR-targeting RPTP, namely DEP-1 (density-enhanced phosphatase-1, also designated CD148, PTP-eta, and PTPRJ). Consistent with the induction of DEP-1 expression in contact-inhibited cells [11], the corresponding gene is often deleted or mutated in carcinomas [12], and DEP-1 exhibits tumor-suppressor activity when ectopically overexpressed [13–16]. Several previous studies identified RTK substrates of DEP-1, including the vascular endothelial growth factor (VEGF) receptor [17–19]. Beyond the unbiased identification of EGFR as a substrate for DEP-1, the results we present shed light on the molecular details of RTK-RPTP interactions: EGFR-DEP complexes exist at the cell surface prior to ligand binding. On binding of EGF, DEP-1 dephosphorylates and thereby stabilizes EGFR and inhibits signaling. Eventually, EGFR undertakes a route leading to endosomes and lysosomes, but DEP-1 remains at the cell surface. The implications of this segregation are discussed in the context of compartmentalized EGFR signaling and the diverse involvement of derailed endocytosis in cancer [20].

Results

An Unbiased Screen Identifies DEP-1 as a Suppressor of EGFR Signaling and Degradation

To substantiate the role of PTPs in EGF-induced phosphorylation events, we treated HeLa cells with two different phosphatase inhibitors and then stimulated them with EGF (Figure 1A).

*Correspondence: yosef.yarden@weizmann.ac.il

⁶These authors contributed equally to this work

⁷Present address: Program in Cell Biology, Hospital for Sick Children, Toronto, ON M5G 1X8, Canada

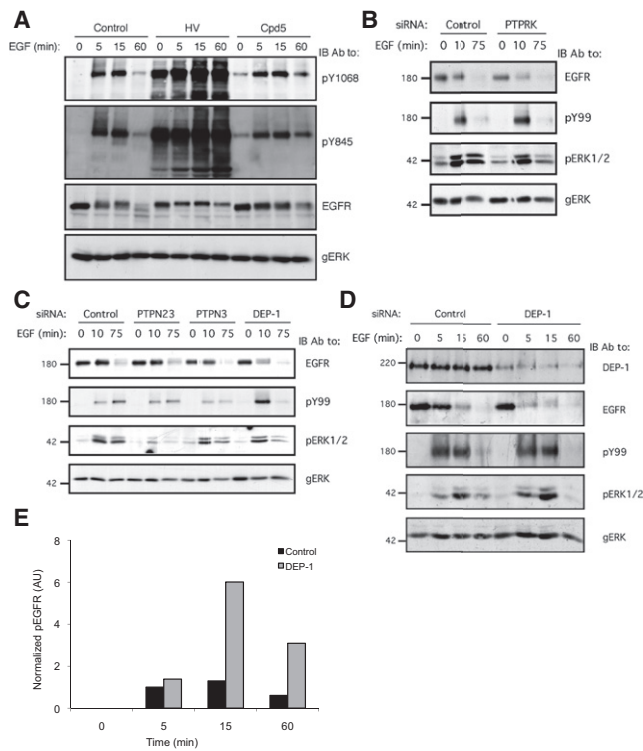


Figure 1. An Unbiased Genetic Screen Identifies Protein Tyrosine Phosphatases Regulating EGF-Mediated Receptor Phosphorylation and Degradation

(A) HeLa cells were serum starved for 16 hr; treated with either a mixture of H₂O₂ (0.2 mM) and sodium orthovanadate (1 mM for 15 min; HV), compound 5 (Cpd5; 20 mM for 30 min), or ethanol (control; 30 min); and then stimulated with EGF (20 ng/ml) for the indicated time intervals. Whole-cell lysates were blotted with the indicated antibodies.

(B and C) Mixtures of siRNA oligonucleotides were transfected into HeLa cells, which were then incubated for 32 hr and serum starved for 16 hr. The cells were then stimulated with EGF (20 ng/ml) for the indicated intervals and were lysed. Whole cell lysates were blotted with the indicated antibodies, including an anti-phosphotyrosine antibody (pY99) and antibodies to the active (pERK) and general (gERK) forms of ERK.

(D) HeLa cells were transiently transfected with DEP-1 siRNA oligonucleotides or with control siRNA (each at 10 nM), incubated for 32 hr, serum starved for 16 hr, and stimulated with EGF (20 ng/ml) for the indicated time intervals. Whole-cell lysates were immunoblotted with the indicated antibodies.

(E) HeLa cells were treated and processed as in (D). EGFR phosphorylation was quantified via densitometric analysis and normalized to total EGFR level. One representative experiment (n = 3) is shown.

A mixture of H₂O₂ and sodium orthovanadate (HV), which potently but nonspecifically inhibits PTPs [21], caused a significant increase in both basal and EGF-induced receptor phosphorylation (Figure 1A). The vitamin K derivative compound 5, a mild inhibitor of PTPs [22], exerted similar but weaker effects (Figure 1A), implying that PTPs critically regulate both basal and EGF-driven receptor phosphorylation.

To identify PTPs that underlie dephosphorylation of EGFR, we screened all human PTPs with a library of siRNA oligonucleotides, collectively targeting 38 PTPs. Pools of four oligonucleotides were transfected into cells, and 48 hr later the cells were stimulated with EGF (see flow diagram in Figure S1 available online). Thereafter, whole-cell lysates were separately immunoblotted with antibodies to EGFR, antibodies to phosphotyrosine (pY99), and antibodies to the active form of

ERK1/2. The library was independently screened twice, and candidates displaying undetectable messenger RNA (mRNA) levels in HeLa cells (Table S1) were eliminated. The screens repeatedly identified PTPRK and DEP-1 (see examples in Figures 1B and 1C). Notably, PTPRK has previously been identified on the basis of coexpressing PTPs together with EGFR in receptor null cells [10], whereas the DEP-1 ortholog of *C. elegans* negatively regulates the worm's EGFR [23].

To validate the knockdown effect of the pool of four siRNA oligonucleotides, collectively targeting DEP-1, we tested individual components, each targeting a distinct part of the DEP-1 transcript. This experiment confirmed that all four independent siRNAs were able to reduce expression of DEP-1 (Figure S2). Next, we transfected HeLa cells with the pool of siRNA oligonucleotides and stimulated them with EGF (Figure 1D). This experiment demonstrated effective siRNA-mediated inhibition of DEP-1 expression and a concomitant enhancement of receptor phosphorylation (peaking at 15 min; Figure 1E). In addition, DEP-1 knockdown accelerated EGFR degradation, and this effect was evident as early as 5 min after EGF stimulation (Figure 1D). By employing commercially available antibodies, which are supposed to recognize specific tyrosine phosphorylation sites of EGFR, we found that depletion of endogenous DEP-1 nonselectively increased receptor phosphorylation, affecting all three sites we analyzed (tyrosines 1045, 1068, and 1173; data not shown). Finally, consistent with enhanced phosphorylation and accelerated degradation of EGFR, we observed in DEP-1-depleted HeLa cells an increase in EGF-stimulated ERK1/2 activation and an earlier decay relative to control cells (Figure 1D).

Knockdown of DEP-1 Enhances Receptor Phosphorylation in Endosomes

To extend the functional analyses of EGFR-DEP-1 interactions to a cellular outcome, we referred to glioblastoma multiforme (GBM), an aggressive brain tumor often presenting overactive EGFRs. As a first step, we screened several GBM cell lines and identified Ln229 cells as high expressors of DEP-1 (Figure 2A). Next, we used siRNA-DEP-1 to achieve effective knockdown. Most importantly, we found that knockdown of DEP-1 resulted in remarkable enhancement of EGFR phosphorylation (Figure 2B), and this was associated with increased cell proliferation (Figure 2C; p = 0.001). These results confirmed that mammalian DEP-1, similar to the invertebrate version, negatively regulates EGFR signaling, which prompted us to analyze the underlying mechanisms.

Our next set of experiments employed siRNA-treated HeLa cells, immunofluorescence, and antibodies specific to EGFR or to phosphorylated tyrosine 1173 (pY1173). As expected, following stimulation with EGF (10 min), the receptor redistributed to endosomes (Figure 2D). Image analyses revealed that the intensity of endosomal pY1173 was elevated in the majority (67%) of siDEP-1-treated cells, as compared to siControl cells (16%; Figures 2D and 2E). Hence, we compared the vesicular pY1173 signal (n ~ 50; >25 cells) in control and DEP-1-depleted cells (Figure 2E). This analysis confirmed that the fraction of pY1173-enriched endosomes was significantly higher in DEP-1-knockdown cells, as compared to control cells (p < 0.001; t test).

In conclusion, depletion of endogenous DEP-1 indicated that the phosphatase normally restricts tyrosine phosphorylation of EGFR, thereby curtailing signaling as well as cellular proliferation and preventing transfer of active receptors to endosomes. This latter observation is consistent with

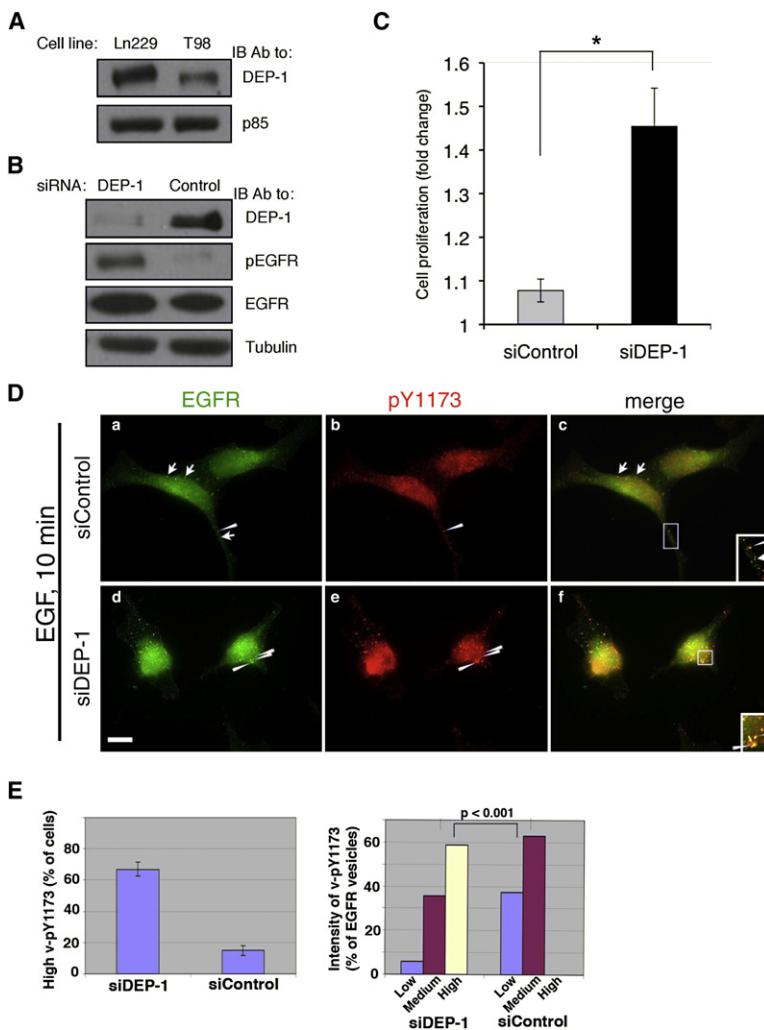


Figure 2. Knockdown of DEP-1 Increases Phosphorylation of Vesicular EGFRs and Enhances Proliferation of Glioblastoma Cells

(A) Whole extracts of Ln229 and T98 glioblastoma cells were immunoblotted with antibodies to DEP-1 or the p85 subunit of phosphoinositide 3-kinase.

(B) Ln229 cells were transfected with siRNA oligonucleotides targeting DEP-1 transcripts. Following 48 hr of incubation, cells were harvested for immunoblotting analysis.

(C) Ln229 cells were transfected with siRNA oligonucleotides targeting DEP-1 transcripts, then incubated for 48 hr and plated in 96-well plates under 1% serum. Proliferation was measured after 3 days and compared to day 1. * $p = 0.001$.

(Da–Df) HeLa cells were transfected with DEP-1-siRNA (10 nM; Dd–Df) or with control siRNA (Da–Dc) and then stimulated with EGF (20 ng/ml, 10 min). Thereafter, cells were analyzed by immunofluorescence with an antibody to EGFR or to phosphorylated EGFR (pY1173). Images were taken at the same exposure time. Arrowheads indicate vesicles positive for both EGFR and pY1173; arrows mark EGFR-positive but pY1173-negative vesicles. Enlarged areas show internalized EGFR in vesicles. Scale bar represents 10 μm . (E) Left: the number of cells displaying >10 pY1173-positive vesicles are compared in DEP-1-siRNA- and control-treated HeLa cells. Data are expressed as mean \pm standard deviation (SD) (bars) of three independent measurements. Right: fluorescence intensities of pY1173-positive vesicles ($n \sim 50$; 5 cells) were analyzed with NIH ImageJ software. The experiment was repeated twice.

a previously inferred receptor inactivation phase affiliated with transfer from the plasma membrane to endosomes [24].

DEP-1 Gain of Function Decreases Signaling Downstream to EGFR and Inhibits Ligand-Induced Receptor Degradation

We next employed ectopic expression of DEP-1 to examine possible reciprocal effects to those reflected by siRNA-treated cells. Forty-eight hours following transfection with a plasmid encoding wild-type (WT), HA (hemagglutinin epitope)-tagged DEP-1, HeLa cells were stimulated with EGF and whole-cell extracts were analyzed (Figures 3A and 3B). DEP-1 overexpression reduced ligand-induced phosphorylation as well as retarded receptor degradation. For example, by 60 min of stimulation, only a small fraction of EGFR escaped degradation; ectopic DEP-1 not only increased this fraction but almost completely erased its tyrosine phosphorylation (Figure 3B). Additionally, the decrease in EGFR activation was followed by decreased activation of ERK1/2 (Figures 3A and 3C). Moreover, the effect of DEP-1 on MAPK activation was reflected in reduced transcription of the *FOS* gene (Figure 3C).

To corroborate a model of DEP-1-enabling escape from degradation, we applied immunofluorescence and WT or a catalytically inactive mutant of DEP-1-HA (C1239S, denoted

CS). Cells were either unstimulated or stimulated with EGF for 10 min, then stained with an antibody to HA or to phosphorylated tyrosine 1173 of EGFR (pY1173; Figure 3D). Ectopic WT-DEP-1 localized to the plasma membrane as well as to polar perinuclear sites, which may correspond to biosynthetic compartments. Unlike unstimulated cells, which displayed very weak pY1173 fluorescence signal (Figures 3Db and 3De), EGF stimulation remarkably increased pY1173 (compare Figures 3Db and 3Dh). Moreover, whereas the pY1173 signal of untransfected cells largely corresponded to endosomes containing the endogenous EGFR of HeLa cells, 95% of WT-DEP-1-expressing cells displayed no (or very weak) punctate pY1173 staining (Figures 3D and 3E). In sharp contrast to WT-DEP-1, vesicular pY1173-EGFR was detectable in most cells expressing the mutant form of the phosphatase (Figures 3Dj–3Di and 3E). Only in a small fraction of CS-DEP-1-expressing cells did we observe a reduction in vesicular pY1173 (Figure 3E), suggesting that DEP-1 strongly inhibits removal of active EGFR molecules from the cell surface into endosomes. In conclusion, the results shown in Figure 3 indicate that DEP-1 can dephosphorylate EGFR at the cell surface; this phosphatase activity is responsible for blocking endocytosis of active receptors and for stabilizing a dephosphorylated form of EGFR at the plasma membrane.

EGFR and DEP-1 Colocalize and Maintain Bidirectional Interactions

The ability of DEP-1 to dephosphorylate EGFR molecules predicted physical interactions that are confined to the cell surface. To test this model, we constructed a mutant of DEP-1 whose conserved aspartate 1205 had been replaced by an alanine (DA mutant), an approach developed for PTP1B [5].

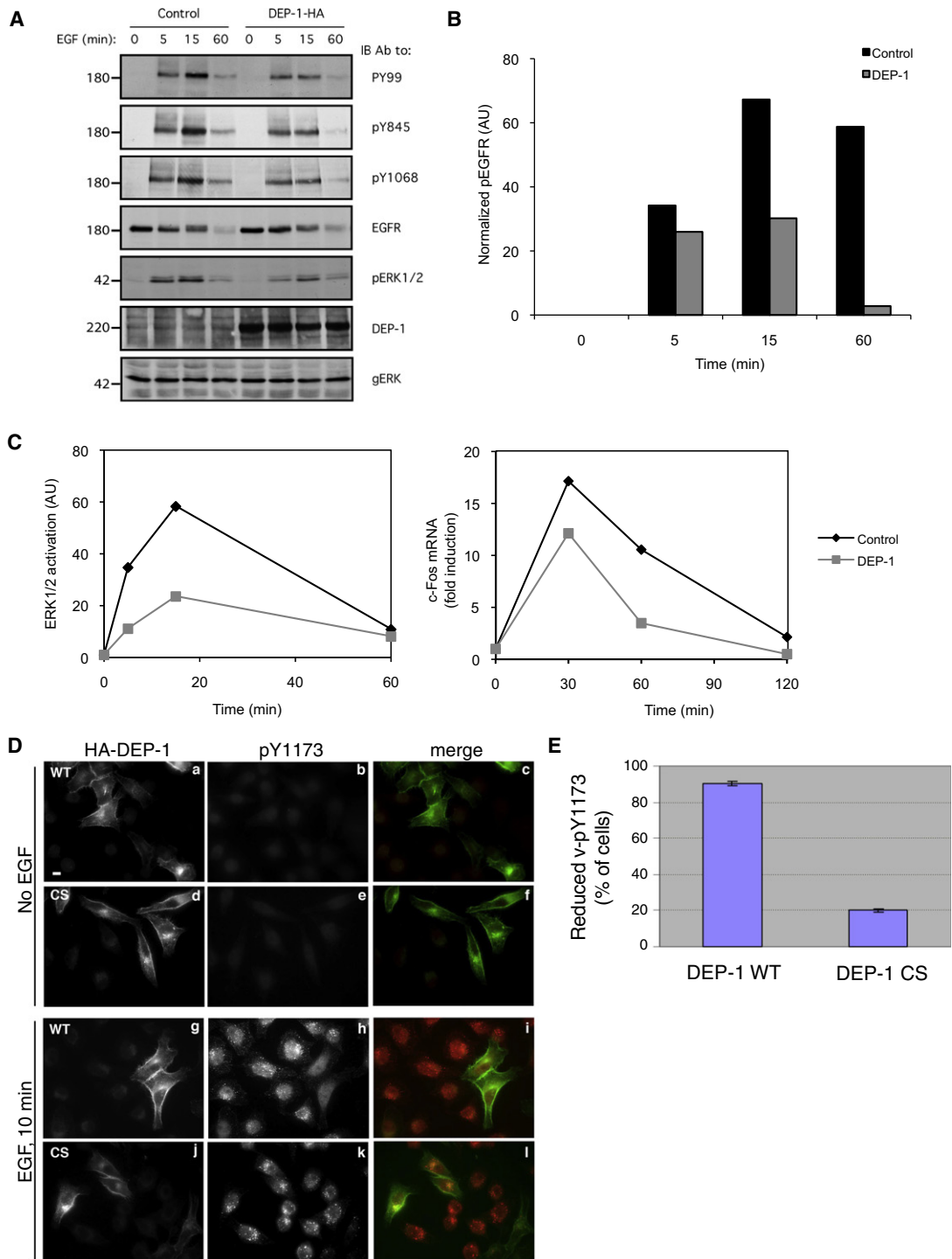


Figure 3. Ectopic DEP-1 Decreases Receptor Phosphorylation, Stabilizes EGFR, and Inhibits Downstream Signaling

(A) HeLa cells were transfected with a plasmid encoding HA (hemagglutinin epitope)-tagged DEP-1 or with a control expression vector and then incubated for 32 hr, serum starved for 16 hr, and stimulated with EGF (20 ng/ml) for the indicated time intervals. Thereafter, cell extracts were analyzed by immunoblotting. (B) HeLa cells were treated as in (A). EGFR phosphorylation was quantified and normalized. One representative experiment ($n = 3$) is shown.

(C) HeLa cells were treated as in (A) and stimulated with EGF (20 ng/ml) for the indicated intervals. Left: cells were processed for immunoblotting and densitometry of pERK1/2 levels (normalized to total ERK2 level; gERK). Right: cells were lysed and total RNA was prepared and used for reverse transcription. Real-time PCR was carried out with *c-FOS* primers.

(D–I) HeLa cells were transfected with plasmids encoding wild-type HA-DEP-1 (Da–Dc and Dg–Di) or a catalytically inactive mutant (CS; Dd–Df and Dj–Dl) and then incubated for 32 hr, serum starved for 16 hr (Da–Df), and stimulated with EGF (20 ng/ml) for 10 min (Dg–Di). Cells were then fixed and analyzed by immunofluorescence with an antibody to HA (Da, Dd, Dg, and Dj) or to phosphorylated EGFR (pY1173; Db, De, Dh, and Dk). Images of phosphorylated EGFR were taken at the same exposure time. Endogenous phosphorylated EGFR appears green; DEP-1 appears red. One representative experiment is shown ($n = 2$). Scale bar represents 10 μ m.

(E) HeLa cells expressing DEP-1 (WT or CS) were treated as in (D). The histogram compares the fractions of cells (\pm SD) displaying vesicular pY1173 in three independent measurements (>100 cells).

Mutagenesis of the invariant catalytic aspartate converts an active enzyme into a “substrate trap.” This mutant did not alter localization of EGFR (Figure 4A), and, like WT-DEP-1 and CS, displayed extensive colocalization with EGFR (Figure 4A). Notably, both proteins localized almost exclusively to the cell surface, and their colocalization was most prominent at cell borders (arrows in Figure 4A).

We next employed a coimmunoprecipitation approach to examine possible physical interactions between EGFR and DEP-1. However, immunoprecipitates of both EGFR and DEP-1 (WT and DA) contained undetectable traces of the other molecule (data not shown), suggesting that, because of rapid turnover of many substrate molecules (i.e., EGFRs) by a single enzyme molecule (i.e., DEP-1), their physical interactions are very weak and transient. Hence, we adopted an *in vitro* assay that employed detergent-solubilized EGFR (from A431 cells) and a bacterially expressed intracellular domain of DEP-1 fused to glutathione S-transferase (GST-DEP-1). Prior to lysis, intact A431 cells were incubated with a radiolabeled EGF and then subjected to covalent crosslinking that enables tagging EGFR with the radioactive ligand [25]. Unlike the WT form of GST-DEP-1, the DA mutant robustly interacted with EGFR (Figure 4B). Two control experiments indicated specific interactions: first, both GST alone and CS displayed no pull-down activity. Second, pretreatment of cells with vanadate, a PTP inhibitor that binds to the catalytic site, reproducibly decreased the signal.

We next asked whether EGFR could transphosphorylate DEP-1 within the constitutive complex. Unlike CS and WT-DEP-1, which displayed no tyrosine phosphorylation upon ectopic expression in HeLa cells, the DA mutant presented weak phosphorylation on tyrosine residues prior to stimulation with EGF (Figure 4C). This signal was reproducibly enhanced following a short (10 min) stimulation with EGF. In line with direct involvement of EGFR’s kinase activity, a specific inhibitor, AG1478, effectively reduced tyrosine phosphorylation of the DA mutant.

Biophysical Measurements of the Noncovalent Interactions between EGFR and DEP-1

To further characterize the nature of the interactions between EGFR and DEP-1, we assayed the efficiency of fluorescence resonance energy transfer (FRET) between fluorescent derivatives, namely EGFR-mRFP and DEP-1-WT-EGFP (or the respective DA and CS mutants), using fluorescence lifetime imaging microscopy (FLIM) as described [26–28]. Because of suboptimal expression of DEP-1-EGFP and EGFR-mRFP, relatively low FRET efficiencies (~4%) were observed in cotransfected HeLa cells. Hence, we used MCF7 mammary cancer cells (Figure 5). The fluorescence lifetime of DEP-1-WT-EGFP and the DA and CS mutants was remarkably reduced by coexpression of EGFR-mRFP, which indicates that FRET occurs between DEP-1-EGFP and EGFR-mRFP (Figures 5A–5C). However, no significant change in FRET signal was detectable upon EGF stimulation in both the WT protein and the CS mutant. Still, DA demonstrated a significant increase in FRET signal upon EGF stimulation (Figures 5B and 5D). These data are consistent with the ability of the DA mutant to bind activated EGFR (Figure 4B), as well as undergo phosphorylation on stimulation with EGF (Figure 4C). In conclusion, the biophysical measurements suggest that DEP-1 and EGFR preexist in a physical complex prior to ligand stimulation. On stimulation, the receptors are better bound by DEP-1 in a rapid

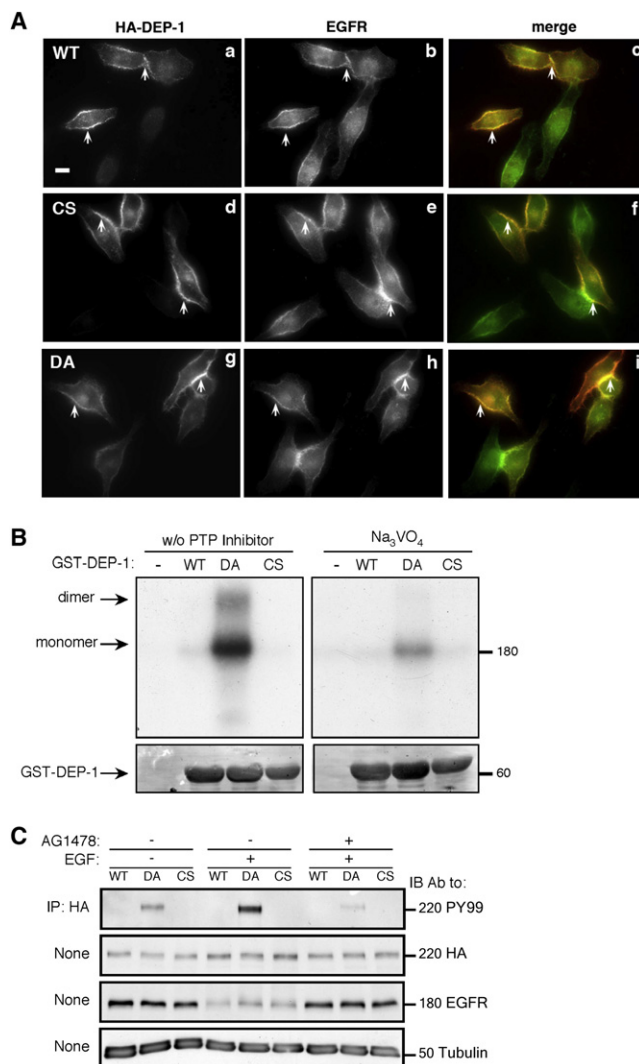


Figure 4. DEP-1 and EGFR Colocalize at the Cell Surface, Physically Interact, and Maintain Bidirectional Enzymatic Interactions

(Aa–Ai) HeLa cells were transiently transfected with vectors encoding HA-tagged WT DEP-1 (Aa–Ac), a CS mutant (Ad–Af), or a DA mutant (Ag–Ai). Thereafter, cells were incubated for 32 hr, serum starved for 16 hr, and fixed. Shown are immunofluorescence images obtained with the indicated antibodies. The merged images (Ac, Af, and Ai) were obtained with the ImageJ Stack RGB Merge plugin and indicate colocalization (yellow) of EGFR (green) and DEP-1 (red). Arrows demarcate colocalization at cell borders and junctions. One representative experiment is shown ($n = 3$). Scale bar represents 10 μm .

(B) A431 cells were incubated for 2 hr at 4°C with a radiolabeled EGF (20 ng/ml) and then washed and subjected to covalent crosslinking with BS³ (1 mM). The crosslinking reaction was subsequently quenched. Cell lysates were mixed, in the absence or presence of sodium orthovanadate (0.2 mM), with glutathione beads bound to purified GST, GST-DEP-1 (WT), DA, or CS mutants and were incubated for 12 hr at 4°C. After extensive washing, the samples were resolved by gel electrophoresis and autoradiography (top panel). Staining with Ponceau red (bottom panel) was used to verify equal gel loading.

(C) HeLa cells were transfected with vectors encoding HA-tagged WT DEP-1 or with the CS or DA mutants. Thereafter, cells were incubated for 32 hr, serum starved for 16 hr, and then preincubated (as indicated) for 30 min with a selective EGFR kinase inhibitor (AG1478; 10 $\mu\text{g/ml}$). This was followed by EGF stimulation (20 ng/ml; 10 min). DEP-1 was immunoprecipitated (IP) from whole-cell lysates with anti-HA-agarose beads, followed by immunoblotting (IB) with the indicated antibodies.

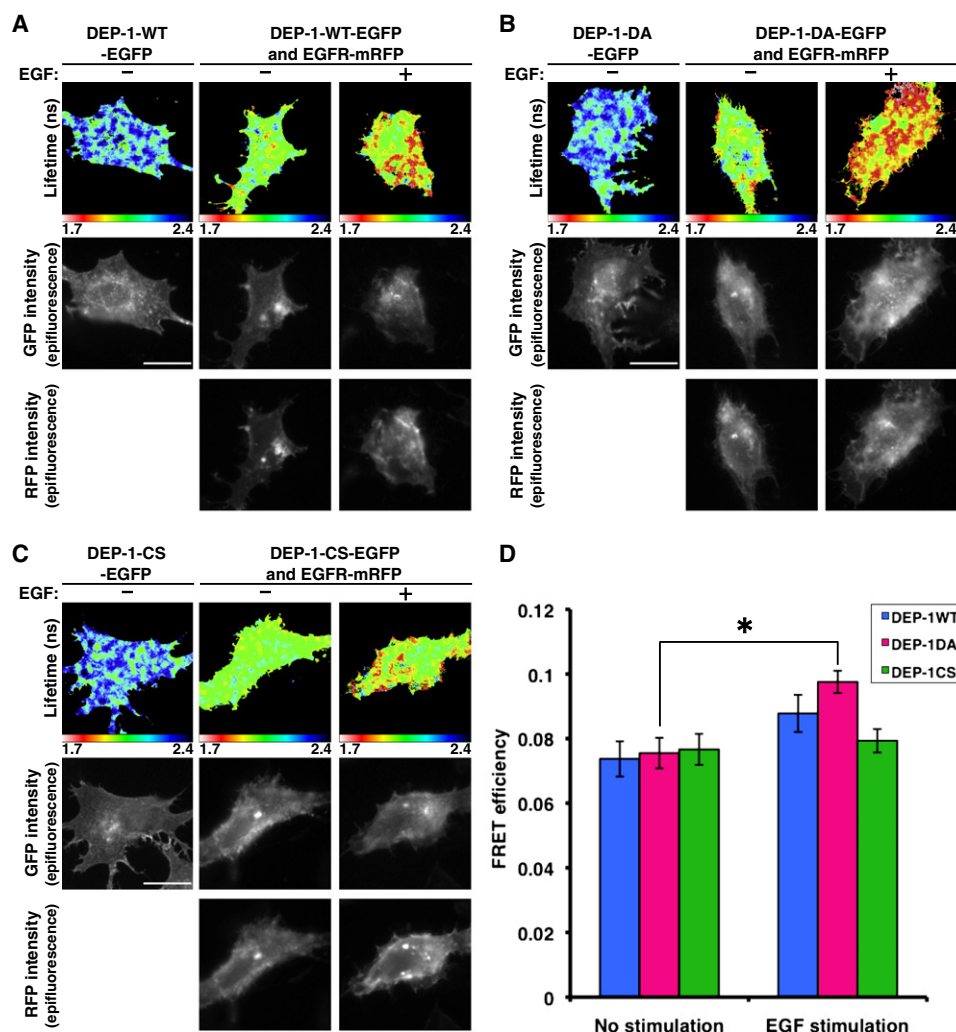


Figure 5. FRET Measurements between DEP-1-EGFP and EGFR-mRFP Show Specific Interactions

(A–C) MCF-7 cells were transfected with vectors encoding EGFR-mRFP, along with GFP-tagged WT DEP-1 (A), the DA mutant (B), or the CS mutant (C). Thereafter, cells were incubated for 32 hr, serum starved for 16 hr, and stimulated with EGF (20 ng/ml; 10 min) prior to fixation and fluorescence measurements. Scale bar represents 20 μ m.

(D) The mean FRET efficiency between DEP-1-EGFP and EGFR-mRFP was calculated with the following equation in each pixel and averaged per each cell. FRET efficiency = $1 - \tau_{da}/\tau_{control}$, where τ_{da} is the lifetime displayed by cells coexpressing both DEP-1-EGFP and EGFR-mRFP, and $\tau_{control}$ is the mean DEP-1-EGFP lifetime measured in the absence of acceptor. Data are means \pm standard error of the mean (SEM) of 16–23 cells from three independent experiments. * $p < 0.05$ for the DA mutant.

and reversible manner, because this increase can only be seen in the presence of a substrate trap (DA) form of DEP-1.

DEP-1 Inhibits EGFR Internalization and Remains at the Cell Surface after EGFR Is Internalized

Because DEP-1-overexpressing cells displayed virtually no tyrosine-phosphorylated EGFRs in endosomes (Figure 3D), we addressed the possibility that the phosphatase inhibits internalization of active EGFRs. Employing flow cytometry, we found that following 10 min of stimulation with EGF, 71.9% of surface EGFR molecules translocated from the surface of siDEP-1-treated cells, as compared to only 47.7% in siControl cells (Figure 6A). Conversely, 52.6% of surface receptors internalized in cells transfected with a control vector, whereas only 30.2% of the receptors underwent internalization in DEP-1-overexpressing cells (Figure 6B). It is notable that only a fraction of HeLa cells undergo transfection.

Hence, signal magnitude and the consistency of these two sets of results clearly indicate that DEP-1 decelerates the rate of ligand-induced EGFR internalization.

Next, we asked whether DEP-1 escorts EGFR to endosomal compartments. To address this question, HeLa cells were stimulated with fluorescently labeled EGF (Figure 6C). Whereas fluorescently labeled EGF efficiently translocated into endosomes, DEP-1 molecules remained at the cell surface (Figure 6C), implying molecular segregation. To further address this scenario, HeLa cells were stimulated with EGF and surface labeled with antibodies to EGFR or to DEP-1, and both surface proteins were quantified by flow cytometry (Figure 6D). As expected, this analysis revealed that 60% of surface-localized EGFR molecules efficiently internalized after 15 min, but essentially all DEP-1 molecules remained at the cell surface. As a final test, we asked whether a fraction of DEP-1 reaches the early endosomal compartment characterized by the

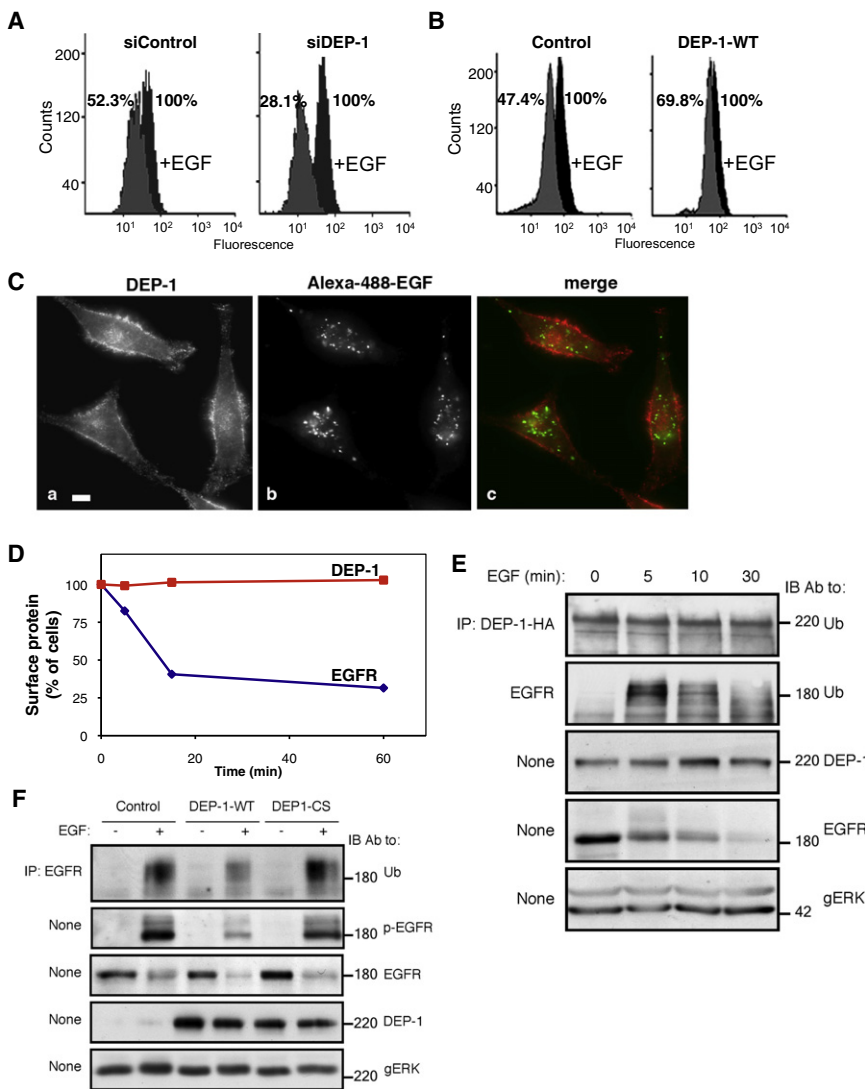


Figure 6. DEP-1 Inhibits EGFR Internalization and Ubiquitylation and Remains on the Cell Surface after EGFR Is Internalized

(A) HeLa cells were transfected with the indicated siRNA oligonucleotides, and 32 hr later they were serum starved for 16 hr and untreated or treated with EGF (20 ng/ml; 10 min). Thereafter, surface-localized EGFR was quantified by flow cytometry. Numbers represent percents of initial cell surface EGFR.

(B) HeLa cells transiently expressing HA-DEP-1 or a control vector were assayed as in (A). One representative experiment ($n = 2$) is shown.

(C) HeLa cells were stimulated with a fluorescently labeled EGF (FITC-EGF; 20 ng/ml) for 30 min at 22°C and fixed and analyzed by immunofluorescence with an antibody to DEP-1.

(D) HeLa cells were serum starved for 16 hr and stimulated with EGF (20 ng/ml) for the indicated time intervals. Thereafter, cells were surface labeled with antibodies to EGFR and DEP-1. The remaining surface fraction of each protein was quantified by flow cytometry.

(E) HeLa cells expressing DEP-1-HA were stimulated with EGF (20 ng/ml) for the indicated time intervals. EGFR and the ectopically expressed DEP-1 were immunoprecipitated from cell lysates and subjected to immunoblotting.

(F) HeLa cells were treated as in (E) and stimulated with EGF (20 ng/ml; 5 min). EGFR was analyzed by immunoblotting, either directly or following immunoprecipitation. EGFR phosphorylation was detected with an anti-phosphotyrosine antibody.

presence of the small GTP-binding protein RAB5. As expected, a RAB5-GFP fusion protein localized to intracellular vesicles, but the coexpressed HA-DEP-1 showed little, if any, colocalization (Figure S3). In conclusion, dephosphorylation by DEP-1 effectively decelerates the rate of EGFR internalization. Eventually, EGFR molecules are internalized, whereas DEP-1 molecules remain at the cell surface, perhaps in order to process other types of RTKs as well as newly delivered EGFR molecules.

DEP-1 Disrupts Physical Association of a Ubiquitin Ligase Complex with EGFR Molecules and Impairs Its Activation

The distinct fates of EGFR and DEP-1 raised the possibility that protein ubiquitylation, which underlies endocytic sorting, would differentiate between the two fates. To test this scenario, we stimulated HeLa cells ectopically expressing WT-DEP-1 with EGF and tested the ubiquitylation status of both EGFR and DEP-1. The results confirmed rapid, EGF-induced ubiquitylation of EGFR (Figure 6E). DEP-1, on the other hand, displayed relatively weak ubiquitylation, which was not affected by EGF, in line with different molecular fates. To test the hypothesis that DEP-1 disrupts receptor ubiquitylation, we expressed it in HeLa cells briefly stimulated with EGF and assessed EGFR ubiquitylation. Whereas the WT

ligase, c-CBL, with EGFR [29]. To test this, we examined the interaction of EGFR with c-CBL, as well as with the CBL's adaptor protein, GRB2 [30]. As predicted, ectopic expression of DEP-1 diminished interactions of EGFR with both c-CBL and GRB2 (Figure 7A). Because c-CBL's activation is achieved via tyrosine phosphorylation, we tested the effect of DEP-1 on modification of a major site of phosphorylation, namely tyrosine 731. Upon DEP-1 overexpression, c-CBL displayed reduced phosphorylation on this site compared to control cells (Figure 7B). This result offers a mechanism by which DEP-1 affects EGFR trafficking: by dephosphorylating EGFR, and possibly also SRC family kinases involved in phosphorylation of c-CBL [31, 32], DEP-1 reduces activation of c-CBL and its recruitment to the activated EGFR, hence inhibiting subsequent receptor internalization and degradation.

In summary, by dephosphorylating EGFR at the cell surface, DEP-1 reduces activation and subsequent recruitment of a dedicated ubiquitin ligase complex (i.e., CBL-GRB2) and inhibits both receptor ubiquitylation and downstream signaling. Consequently, surface-localized receptors undergo inactivation, their translocation to endosomes is delayed, and those receptors that eventually reach the endocytic compartment are largely disarmed (see model in Figure 7C).

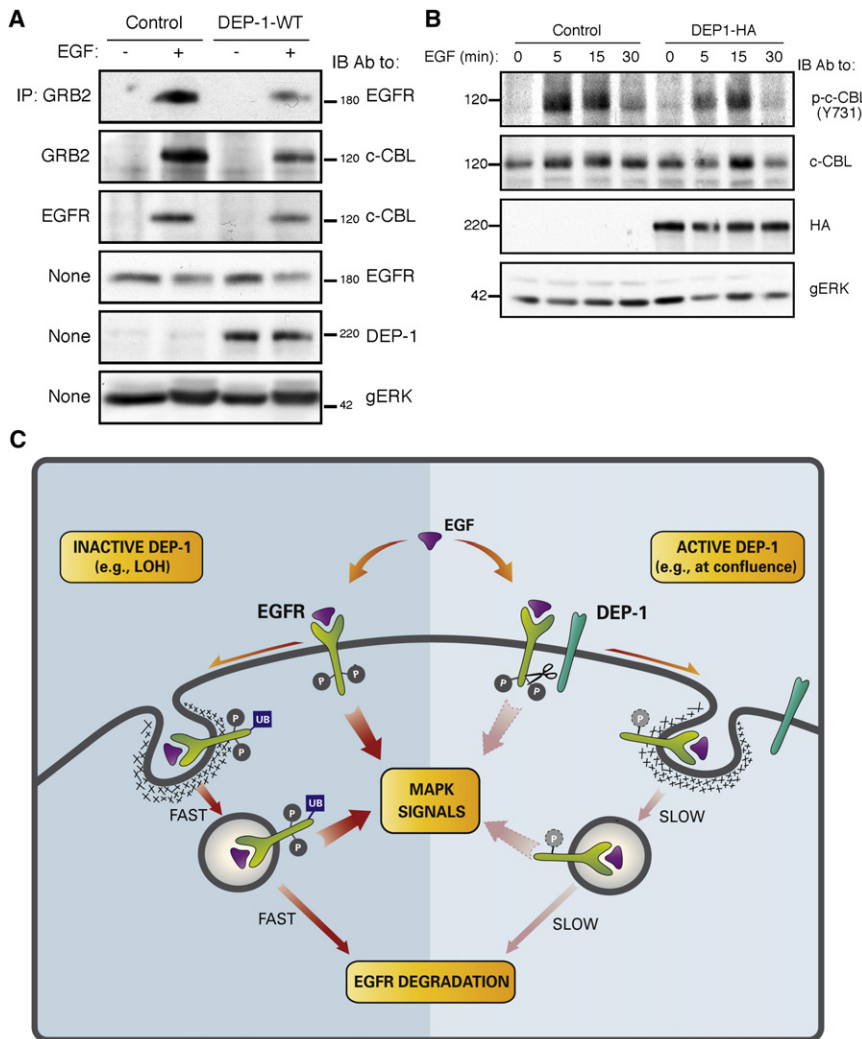


Figure 7. DEP-1 Disrupts Physical Association of a Ubiquitin Ligase Complex with EGFR Molecules and Impairs Its Activation

(A and B) HeLa cells were transfected with control or DEP-1-HA plasmids, incubated for 32 hr, serum starved for 16 hr, and stimulated with EGF (20 ng/ml) for either 5 min (A) or for the indicated time intervals. Whole cell lysates were immunoblotted with the indicated antibodies.

(C) Model presenting the effect of DEP-1 on EGFR signaling and endocytosis: a complex comprising EGFR and DEP-1 preexists at the surface, especially in highly confluent epithelia. On EGF binding and receptor phosphorylation (P), DEP-1 dephosphorylates EGFR, thereby inhibiting receptor ubiquitylation (Ub) by c-CBL, which decelerates the rate of receptor internalization and diminishes MAPK signals generated at the membrane and in endosomes. When DEP-1 is inactive, as a result of heterozygosity (LOH), for example, EGFR is hyperphosphorylated and accordingly relays strong signals to MAPK, although it gains fast rates of internalization and degradation.

of EGFR in mammalian cells [10] and as an enzyme whose invertebrate ortholog genetically interacts with EGFR of *C. elegans* [23]. Several other screening strategies have previously been employed, including the utilization of substrate-trapping mutants, which identified PTP-1B [6] and TC-PTP [7] as EGFR regulators. The latter enzyme mediates suppression of EGFR by integrins [9], suggesting that screening assays performed on distinct extracellular matrices may identify different enzymes.

Here we demonstrate that DEP-1 suppresses growth signals initiated by EGFR (Figure 2C). Likewise, previous reports documented an ability of DEP-1 to suppress signals emanating from other RTKs, such as PDGF-beta receptors [35], VEGF receptors [17], and c-Met/HGF receptor [19]. Taken together with our results, these observations suggest that DEP-1 acts as a pan-RTK suppressor of growth-factor signals. In combination with pan-RTK functions, our results attribute suppression of tumorigenesis to the ability of DEP-1 to dephosphorylate EGFR and to concurrently inhibit receptor translocation to endosomes and to the nucleus, compartments believed to support long-term RTK signaling [36]. Supporting lines of evidence include the ability of an overexpressed DEP-1 to induce differentiation and suppress tumor cell growth [14, 15]. In the same vein, a transforming acute retrovirus reduces DEP-1 expression [37], and conversely, forced expression of DEP-1 suppresses transformation by viral oncogenes [15]. Finally, the gene encoding DEP-1 has been identified as a candidate for a murine colon cancer susceptibility locus (SCC1 [12]). Loss of heterozygosity (LOH) of the human gene is frequently found in colon, breast [38], and thyroid [39] cancer.

Although no previous study associated DEP-1 with a defect in the transfer of active receptors to endosomes, several published findings, such as DEP-1-mediated reduction in MAPK signaling [40] as well as stabilization of the cell cycle inhibitor

Discussion

By employing an unbiased screen of all human PTPs, we identified DEP-1/PTPRJ as a phosphatase acting on EGFR. Because EGFR drives several types of malignancies in human (reviewed in [2]) and DEP-1 acts as a suppressor of several human tumors, including colon, lung, breast [12], and thyroid [33] cancer, these observations shed new light on the molecular mechanisms enabling DEP-1 to exert tumor-suppressive activities. Similarly important is the finding that DEP-1 inhibits both receptor activation at the plasma membrane and transfer of active receptors to endosomes while it remains confined to the cell surface (see model in Figure 7C). These findings explain the previously observed inactivation-reactivation sequel of EGFR while en route to endosomes [24], and they also illuminate from a new perspective existing models attributing signaling capabilities to endosomal EGFRs [34].

RTKs Provide a Potential Mechanistic Basis for Tumor Suppression by DEP-1

Our screening strategy represents the first exhaustive search for PTPs specific to EGFR. In support of the reliability of our strategy, the two enzymes we identified, namely RPTP-kappa and DEP-1, have respectively been reported as a regulator

p21-KIP1 [15], are consistent with a mechanism involving inhibition of signals emanating from both the plasma membrane and intracellular compartments. When combined with the reported ability of DEP-1 to mediate contact inhibition of cell growth [11], our results suggest the following explanation for the tumor-suppressive activity of DEP-1: by dephosphorylating EGFR at the plasma membrane and by halting transfer of active receptors to intracellular sites of signal generation, DEP-1 confers contact inhibition of cell growth. Once this activity of DEP-1 is compromised by LOH or by other mechanisms, epithelial cells are free to fully respond to EGF and to other growth factors (e.g., HGF and VEGF), thus promoting cell proliferation, migration, and recruitment of blood vessels essential for tumor progression.

Functional Implications of the Ability of DEP-1 to Inhibit Endocytosis of EGFR

By injecting EGF into the portal vein of rats and analyzing hepatic plasma membrane and endosomal fractions, Bergeron and colleagues inferred a pre-endocytosis desensitization step [24]. They later found that the endosomal tyrosine-phosphorylated receptors nucleate a signaling complex containing SHC and the RAS guanine nucleotide exchange factor mSOS [41]. Similarly, other researchers identified a pool of active, ligand-bound PDGF-beta receptors in endosomes [42]. These studies, along with a large series of analyses addressing the nerve growth factor receptor, led to the realization that the RTK-harboring endosome serves as a platform for signal transduction events [34]. In view of the strict compartmentalization of DEP-1 to the plasma membrane and the segregation from internalizing receptors, the concept of "signaling endosomes" may be revised as follows: while at the plasma membrane, activation of RTKs like EGFR is tightly controlled by DEP-1. However, upon translocation to endosomes and segregation from DEP-1, receptor autophosphorylation is relieved, which licenses endosomal signaling.

In summary, our study has identified a novel RTK regulatory pathway: by dephosphorylating EGFR at the plasma membrane and limiting endocytosis of active receptors, DEP-1 tightly controls EGFR's ability to generate intracellular signals. This regulatory pathway plays an important role during embryonic development of invertebrates [23], and it is manipulated in human carcinomas, whose DEP-1 frequently undergoes genetic alterations [12, 38]. Future studies will address the relevance of the DEP-1 regulatory module to other pairs of RTKs and the respective receptor-like PTPs.

Experimental Procedures

Reagents and Antibodies

Monoclonal antibodies to EGFR were from Upstate Biotechnology, Alexis Biotechnology, or were generated in our laboratory. Antibodies to specific phosphotyrosines of EGFR were from Cell Signaling or Zymed. Other antibodies were from R&D Systems (DEP-1), Babco (ubiquitin), Roche (hemagglutinin), Jackson ImmunoResearch Laboratories (Cy2-conjugated), or Santa Cruz Biotechnology. EGF conjugated to Alexa Fluor 488 streptavidin was from Molecular Probes.

Cellular Treatments and Transfection

Transient plasmid expression was achieved with the jetPEI transfection reagent (Polyplus-transfection). siRNA transfection was carried out with HiPerFect Transfection Reagent (QIAGEN). Delivery effectiveness of siRNA was determined with the KDalert GAPDH Assay Kit (Ambion).

Expression Vectors and siRNA Oligonucleotides

Plasmids (pSR α) encoding HA-tagged DEP-1 (wild-type [WT], C1239S [CS], and D1205A [DA]) have been described [43]. EGFP-tagged DEP-1 was a kind gift from A. Östman. siDEP-1 and control siRNA oligonucleotides were obtained from Dharmacon (DEP-1; accession number M-008476-01, siControl; accession number D-001206-14; Table S2). RAB5-GFP was a kind gift of S. Lev.

Real-Time Quantitative PCR

cDNA was generated using the SuperScript First-Strand Synthesis kit (Invitrogen). Real-time PCR analysis was performed using the DyNamo HS SYBR Green qPCR Kit (Finnzymes). All experiments were carried out in triplicates and normalized to beta-2 microglobulin RNA levels.

Immunoblotting, Immunoprecipitation, and Pull-down Analyses

The procedures and content of buffers were essentially as described [29]. For pull-down, radiolabeled EGF (20 ng/ml) was incubated for 2 hr at 4°C with confluent A431 cells (10⁷ cells). Following extensive washing, saline containing bis(succinimidyl) suberate (BS³; 1 mM) was incubated with the cells for 20 min at room temperature. The reagent was quenched in quenching solution (10 mM Tris-HCl [pH 7.5], 200 mM glycine, and 2 mM EDTA). Cells were harvested in saline and solubilized in the absence or presence of 0.2 mM sodium orthovanadate. Subsequently, glutathione beads bound to different GST proteins (0.05 mg each) were added, and the mixtures were rotated for 12 hr at 4°C prior to washing and gel electrophoresis.

Immunofluorescence

Cells were treated as described [44]. Images of fixed cells were recorded with a DeltaVision system (Applied Precision) that included an Olympus IX71 inverted fluorescence microscope equipped with a charge-coupled camera (Photometrics), a 100 W mercury lamp, and excitation and emission filter wheels. Images were acquired with an Olympus Plan ApoN 60 \times 1.42 NA objective. pY1173 fluorescence intensity of EGFR-positive vesicles was determined by calculating the mean gray value within the selected vesicular areas. Fluorescence intensity was measured using a VICTOR2 Multilabel Counter (PerkinElmer).

Cell Proliferation Assay

Cells grown in Dulbecco's modified Eagle's medium supplemented with 10% fetal bovine serum were transfected with siRNA nucleotides (25 nM) obtained from Applied Biosystems (DEP-1; catalog # S230208 and scrambled; catalog #AM4611). After 48 hr, cells were replated in 96-well plates, and, following an overnight incubation, media were changed to 1% serum; relative cell proliferation was measured on day 0 and day 3 using the WST-1 Kit from Chemicon.

Flow Cytometry

Flow cytometry was carried out as described [45].

FRET Determination by Multiphoton FLIM Measurements

FLIM was performed with a custom-built multiphoton system constructed around an upright 90i fluorescence microscope (Nikon) and similar to that described elsewhere [46].

Supplemental Data

Supplemental Data include three figures and two tables and can be found online at [http://www.cell.com/current-biology/supplemental/S0960-9822\(09\)01761-8](http://www.cell.com/current-biology/supplemental/S0960-9822(09)01761-8).

Acknowledgments

We thank G. Gur and A. Elson for insightful comments and A. Östman for reagents. Y.Y. is the incumbent of the Harold and Zelda Goldenberg Professorial Chair. This work was supported by research grants from the US National Cancer Institute (CA072981), the Israel Science Foundation, the Dr. Miriam and Sheldon G. Adelson Medical Research Foundation, and the German-Israeli Foundation. T.K. is supported by King's College London Breakthrough Research Unit funding.

Received: June 17, 2009

Revised: September 15, 2009

Accepted: September 15, 2009

Published online: October 15, 2009

References

1. Tonks, N.K. (2006). Protein tyrosine phosphatases: From genes, to function, to disease. *Nat. Rev. Mol. Cell Biol.* 7, 833–846.
2. Citri, A., and Yarden, Y. (2006). EGF-ERBB signaling: Towards the systems level. *Nat. Rev. Mol. Cell Biol.* 7, 505–516.
3. Katzmann, D.J., Odorizzi, G., and Emr, S.D. (2002). Receptor downregulation and multivesicular-body sorting. *Nat. Rev. Mol. Cell Biol.* 3, 893–905.
4. Suarez Pestana, E., Tenev, T., Gross, S., Stoyanov, B., Ogata, M., and Bohmer, F.D. (1999). The transmembrane protein tyrosine phosphatase RPTPsigma modulates signaling of the epidermal growth factor receptor in A431 cells. *Oncogene* 18, 4069–4079.
5. Flint, A.J., Tiganis, T., Barford, D., and Tonks, N.K. (1997). Development of “substrate-trapping” mutants to identify physiological substrates of protein tyrosine phosphatases. *Proc. Natl. Acad. Sci. USA* 94, 1680–1685.
6. Liu, F., and Chernoff, J. (1997). Protein tyrosine phosphatase 1B interacts with and is tyrosine phosphorylated by the epidermal growth factor receptor. *Biochem. J.* 327, 139–145.
7. Tiganis, T., Bennett, A.M., Ravichandran, K.S., and Tonks, N.K. (1998). Epidermal growth factor receptor and the adaptor protein p52Shc are specific substrates of T-cell protein tyrosine phosphatase. *Mol. Cell Biol.* 18, 1622–1634.
8. Reynolds, A.R., Tischer, C., Verveer, P.J., Rocks, O., and Bastiaens, P.I. (2003). EGFR activation coupled to inhibition of tyrosine phosphatases causes lateral signal propagation. *Nat. Cell Biol.* 5, 447–453.
9. Mattila, E., Pellinen, T., Nevo, J., Vuoriluoto, K., Arjonen, A., and Ivaska, J. (2005). Negative regulation of EGFR signaling through integrin- α 1 β 1-mediated activation of protein tyrosine phosphatase TCPTP. *Nat. Cell Biol.* 7, 78–85.
10. Xu, Y., Tan, L.J., Grachtchouk, V., Voorhees, J.J., and Fisher, G.J. (2005). Receptor-type protein-tyrosine phosphatase-kappa regulates epidermal growth factor receptor function. *J. Biol. Chem.* 280, 42694–42700.
11. Ostman, A., Yang, Q., and Tonks, N.K. (1994). Expression of DEP-1, a receptor-like protein-tyrosine-phosphatase, is enhanced with increasing cell density. *Proc. Natl. Acad. Sci. USA* 91, 9680–9684.
12. Ruivenkamp, C.A., van Wezel, T., Zanon, C., Stassen, A.P., Vceck, C., Csikos, T., Klous, A.M., Tripodis, N., Perrakis, A., Boerigter, L., et al. (2002). Ptpnj is a candidate for the mouse colon-cancer susceptibility locus Sccl and is frequently deleted in human cancers. *Nat. Genet.* 31, 295–300.
13. Iuliano, R., Trapasso, F., Le Pera, I., Schepis, F., Sama, I., Clodomiro, A., Dumon, K.R., Santoro, M., Chiariotti, L., Viglietto, G., et al. (2003). An adenovirus carrying the rat protein tyrosine phosphatase eta suppresses the growth of human thyroid carcinoma cell lines in vitro and in vivo. *Cancer Res.* 63, 882–886.
14. Keane, M.M., Lowrey, G.A., Ettenberg, S.A., Dayton, M.A., and Lipkowitz, S. (1996). The protein tyrosine phosphatase DEP-1 is induced during differentiation and inhibits growth of breast cancer cells. *Cancer Res.* 56, 4236–4243.
15. Trapasso, F., Iuliano, R., Boccia, A., Stella, A., Visconti, R., Bruni, P., Baldassarre, G., Santoro, M., Viglietto, G., and Fusco, A. (2000). Rat protein tyrosine phosphatase eta suppresses the neoplastic phenotype of retrovirally transformed thyroid cells through the stabilization of p27(Kip1). *Mol. Cell Biol.* 20, 9236–9246.
16. Trapasso, F., Yendamuri, S., Dumon, K.R., Iuliano, R., Cesari, R., Feig, B., Seto, R., Infante, L., Ishii, H., Vecchione, A., et al. (2004). Restoration of receptor-type protein tyrosine phosphatase eta function inhibits human pancreatic carcinoma cell growth in vitro and in vivo. *Carcinogenesis* 25, 2107–2114.
17. Grazia Lampugnani, M., Zanetti, A., Corada, M., Takahashi, T., Balconi, G., Breviario, F., Orsenigo, F., Cattelino, A., Kemler, R., Daniel, T.O., et al. (2003). Contact inhibition of VEGF-induced proliferation requires vascular endothelial cadherin, beta-catenin, and the phosphatase DEP-1/CD148. *J. Cell Biol.* 161, 793–804.
18. Jandt, E., Denner, K., Kovalenko, M., Ostman, A., and Bohmer, F.D. (2003). The protein-tyrosine phosphatase DEP-1 modulates growth factor-stimulated cell migration and cell-matrix adhesion. *Oncogene* 22, 4175–4185.
19. Palka, H.L., Park, M., and Tonks, N.K. (2003). Hepatocyte growth factor receptor tyrosine kinase met is a substrate of the receptor protein-tyrosine phosphatase DEP-1. *J. Biol. Chem.* 278, 5728–5735.
20. Mosesson, Y., Chetrit, D., Schley, L., Berghoff, J., Ziv, T., Carvalho, S., Milanezi, F., Admon, A., Schmitt, F., Ehrlich, M., et al. (2009). Monoubiquitylation regulates endosomal localization of Lst2, a negative regulator of EGF receptor signaling. *Dev. Cell* 16, 687–698.
21. Gordon, J.A. (1991). Use of vanadate as protein-phosphotyrosine phosphatase inhibitor. *Methods Enzymol.* 201, 477–482.
22. Onoda, T., Iinuma, H., Sasaki, Y., Hamada, M., Isshiki, K., Naganawa, H., Takeuchi, T., Tatsuta, K., and Umezawa, K. (1989). Isolation of a novel tyrosine kinase inhibitor, lavendustin A, from *Streptomyces griseola-vendus*. *J. Nat. Prod.* 52, 1252–1257.
23. Berset, T.A., Hoier, E.F., and Hajnal, A. (2005). The *C. elegans* homolog of the mammalian tumor suppressor Dep-1/Sccl inhibits EGFR signaling to regulate binary cell fate decisions. *Genes Dev.* 19, 1328–1340.
24. Lai, W.H., Cameron, P.H., Doherty, J.J., 2nd, Posner, B.I., and Bergeron, J.J. (1989). Ligand-mediated autophosphorylation activity of the epidermal growth factor receptor during internalization. *J. Cell Biol.* 109, 2751–2760.
25. Goldman, R., Levy, R.B., Peles, E., and Yarden, Y. (1990). Heterodimerization of the erbB-1 and erbB-2 receptors in human breast carcinoma cells: A mechanism for receptor transregulation. *Biochemistry* 29, 11024–11028.
26. Legg, J.W., Lewis, C.A., Parsons, M., Ng, T., and Isacke, C.M. (2002). A novel PKC-regulated mechanism controls CD44 ezrin association and directional cell motility. *Nat. Cell Biol.* 4, 399–407.
27. Ng, T., Squire, A., Hansra, G., Bornancin, F., Prevostel, C., Hanby, A., Harris, W., Barnes, D., Schmidt, S., Mellor, H., et al. (1999). Imaging protein kinase C α activation in cells. *Science* 283, 2085–2089.
28. Barber, P.R., Ameer-Beg, S.M., Gilbey, J., Carlin, L.M., Keppler, M., Ng, T.C., and Vojnovic, B. (2009). Multiphoton time-domain fluorescence lifetime imaging microscopy: Practical application to protein-protein interactions using global analysis. *J. R. Soc. Interface* 6, S93–S105.
29. Levkowitz, G., Waterman, H., Ettenberg, S.A., Katz, M., Tsygankov, A.Y., Alroy, I., Lavi, S., Iwai, K., Reiss, Y., Ciechanover, A., et al. (1999). Ubiquitin ligase activity and tyrosine phosphorylation underlie suppression of growth factor signaling by c-Cbl/Sli-1. *Mol. Cell* 4, 1029–1040.
30. Waterman, H., and Yarden, Y. (2001). Molecular mechanisms underlying endocytosis and sorting of ErbB receptor tyrosine kinases. *FEBS Lett.* 490, 142–152.
31. Feshchenko, E.A., Langdon, W.Y., and Tsygankov, A.Y. (1998). Fyn, Yes, and Syk phosphorylation sites in c-Cbl map to the same tyrosine residues that become phosphorylated in activated T cells. *J. Biol. Chem.* 273, 8323–8331.
32. Pera, I.L., Iuliano, R., Florio, T., Susini, C., Trapasso, F., Santoro, M., Chiariotti, L., Schettini, G., Viglietto, G., and Fusco, A. (2005). The rat tyrosine phosphatase eta increases cell adhesion by activating c-Src through dephosphorylation of its inhibitory phosphotyrosine residue. *Oncogene* 24, 3187–3195.
33. Iervolino, A., Iuliano, R., Trapasso, F., Viglietto, G., Melillo, R.M., Carlomagno, F., Santoro, M., and Fusco, A. (2006). The receptor-type protein tyrosine phosphatase J antagonizes the biochemical and biological effects of RET-derived oncoproteins. *Cancer Res.* 66, 6280–6287.
34. Polo, S., and Di Fiore, P.P. (2006). Endocytosis conducts the cell signaling orchestra. *Cell* 124, 897–900.
35. Kovalenko, M., Denner, K., Sandstrom, J., Persson, C., Gross, S., Jandt, E., Vilella, R., Bohmer, F., and Ostman, A. (2000). Site-selective dephosphorylation of the platelet-derived growth factor beta-receptor by the receptor-like protein-tyrosine phosphatase DEP-1. *J. Biol. Chem.* 275, 16219–16226.
36. Miaczynska, M., Christoforidis, S., Giner, A., Shevchenko, A., Uttenweiller-Joseph, S., Habermann, B., Wilm, M., Parton, R.G., and Zerial, M. (2004). APPL proteins link Rab5 to nuclear signal transduction via an endosomal compartment. *Cell* 116, 445–456.
37. Zhang, L., Martelli, M.L., Battaglia, C., Trapasso, F., Tramontano, D., Viglietto, G., Porcellini, A., Santoro, M., and Fusco, A. (1997). Thyroid cell transformation inhibits the expression of a novel rat protein tyrosine phosphatase. *Exp. Cell Res.* 235, 62–70.
38. Ruivenkamp, C., Hermsen, M., Postma, C., Klous, A., Baak, J., Meijer, G., and Demant, P. (2003). LOH of PTPRJ occurs early in colorectal cancer and is associated with chromosomal loss of 18q12–21. *Oncogene* 22, 3472–3474.
39. Iuliano, R., Le Pera, I., Cristofaro, C., Baudi, F., Arturi, F., Pallante, P., Martelli, M.L., Trapasso, F., Chiariotti, L., and Fusco, A. (2004). The

tyrosine phosphatase PTPRJ/DEP-1 genotype affects thyroid carcinogenesis. *Oncogene* 23, 8432–8438.

40. Sacco, F., Tinti, M., Palma, A., Ferrari, E., Nardoza, A.P., Hooft van Huijsduijnen, R., Takahashi, T., Castagnoli, L., and Cesareni, G. (2009). Tumor suppressor density-enhanced phosphatase-1 (DEP-1) inhibits the RAS pathway by direct dephosphorylation of ERK1/2 kinases. *J Biol Chem.* 284, 22048–22058.
41. Di Guglielmo, G.M., Baass, P.C., Ou, W.J., Posner, B.I., and Bergeron, J.J. (1994). Compartmentalization of SHC, GRB2 and mSOS, and hyperphosphorylation of Raf-1 by EGF but not insulin in liver parenchyma. *EMBO J.* 13, 4269–4277.
42. Sorkin, A., Eriksson, A., Heldin, C.H., Westermark, B., and Claesson-Welsh, L. (1993). Pool of ligand-bound platelet-derived growth factor beta-receptors remain activated and tyrosine phosphorylated after internalization. *J. Cell. Physiol.* 156, 373–382.
43. Tsuboi, N., Utsunomiya, T., Roberts, R.L., Ito, H., Takahashi, K., Noda, M., and Takahashi, T. (2008). The tyrosine phosphatase CD148 interacts with p85 regulatory subunit of phosphoinositide 3-kinase. *Biochem J.* 413, 193–200.
44. Katz, M., Shtiegman, K., Tal-Or, P., Yakir, L., Mosesson, Y., Harari, D., Machluf, Y., Asao, H., Jovin, T., Sugamura, K., et al. (2002). Ligand-independent degradation of epidermal growth factor receptor involves receptor ubiquitylation and Hgs, an adaptor whose ubiquitin-interacting motif targets ubiquitylation by Nedd4. *Traffic* 3, 740–751.
45. Zwang, Y., and Yarden, Y. (2006). p38 MAP kinase mediates stress-induced internalization of EGFR: Implications for cancer chemotherapy. *EMBO J.* 25, 4195–4206.
46. Peter, M., Ameer-Beg, S.M., Hughes, M.K., Keppler, M.D., Prag, S., Marsh, M., Vojnovic, B., and Ng, T. (2005). Multiphoton-FLIM quantification of the EGFP-mRFP1 FRET pair for localization of membrane receptor-kinase interactions. *Biophys. J.* 88, 1224–1237.